Effect of chemical composition and plastic deformation on corrosion properties of high-Mn austenitic steels in alkaline solution

A. Kozłowska*, A. Grajcar

Division of Constructional and Special Materials, Institute of Engineering Materials and Biomaterials, Silesian University of Technology, ul. Konarskiego 18a, 44-100 Gliwice, Poland

* Corresponding e-mail address: aleksandra.kozlowska@polsl.pl

ABSTRACT

Purpose: The aim of the paper is to compare the corrosion properties of two high-Mn austenitic steels with various Al and Si additions in 0.1M NaOH solution using a potentiodynamic method.

Design/methodology/approach: The steels used for the investigation were thermo-mechanically rolled in 3 passes. The final thickness of about 2 mm was obtained at a temperature of 850°C. Three groups of samples were prepared: thermomechanically rolled, thermomechanically rolled and additionally annealed at 900°C for 20 min, thermomechanically rolled and additionally cold deformed in static tensile test to total elongation of 36%. Corrosion resistance of investigated steels was examined using the potentiodynamic method. The metallographic inspection of corrosion damage included scanning electron microscope observations. The chemical analyses of the corrosion pits were carried out using EDS techniques.

Findings: It was found that X4MnSiAlNbTi27-4-2 and X6MnSiAlNbTi26-3-3 steels were characterized by relatively high corrosion resistance in 0.1M NaOH solution independently of their state. EDS analysis revealed that corrosion pits nucleated preferentially at non-metallic inclusions such as MnS and AlN. Results of potentiodynamic tests showed that cold deformation had the highest influence on decreasing the corrosion resistance of investigated steels. Thermomechanically treated and supersaturated specimens showed lower values of corrosion current density and consequently less amount of corrosion damage.

Research limitations/implications: To investigate in more detail the corrosion behaviour of high-manganese austenitic steels, the impedance spectroscopy investigations will be carried out.

Practical implications: The knowledge of the corrosion resistance of high-Mn steels has a significant effect on their industrial application in the automotive industry.

Originality/value: The corrosion resistance of two high-manganese austenitic steels with different initial microstructures was compared in alkaline solution.

Keywords: Corrosion resistance; High-manganese steel; Non-metallic inclusion; Potentiodynamic test; Pitting corrosion

PROPERTIES

1. Introduction

High-manganese austenitic steels belong to the second generation of advanced high strength steels (AHSS) dedicated for automotive industry. These steels are being developed as structural material due to their superior combination of strength, ductility and crashworthiness. Their applications include different structural elements with a complicated shape used in the crumple zones of cars [1-4]. In addition to the automotive industry the high-Mn steels can be used as replacements for traditional Cr-Ni steels for transportation of liquid gases due to their high strength and toughness at cryogenic temperatures. Excellent mechanical properties are related to homogenous austenitic microstructure. These steels contain manganese (15-30%) which is known as a major austenite stabilizer. The other alloying elements like aluminium and silicon also play a role in the physical and mechanical behaviour of high-manganese steels. Silicon and aluminium additions provide solid solution strengthening. Microadditions of Nb and Ti are added for precipitation strengthening and grain refinement [5]. Manufacturing methods of high-manganese steels consist of hot-rolling and successive cooling to room temperature [6].

Chemical composition, heat treatment and plastic deformation as well as a type of corrosive media have significant effects on the corrosion properties of high-Mn steels. It was found that additions of Al, Cr, Cu and Mo improve corrosion resistance of these steels due to the passive film formation on a steel surface. Silicon addition has a negative effect on the corrosion resistance of steels [7,8]. Our previous studies [9,10] demonstrated that a presence of sulfide compounds, especially MnS inclusions, affects the corrosion resistance of steel by providing pitting sites. The same effect was observed in stainless steels by other authors [11-13]. Manganese occurs also with silicon and aluminium additions characterized by high affinity to oxygen (aluminium also to nitrogen). Results of our previous works [9,10] showed that corrosion pits were formed at complex inclusions such as MnS+AlN, oxysulphides containing Mn, Al, N, Si and oxides containing Mn, Al, Si.

A type of corrosive medium affects corrosion resistance of steels. It was reported that high-Mn steels show the lowest corrosion resistance in solutions of pH about 1 [14-16]. These steels are less sensitive to corrosion attack in solutions of pH about 14. In our previous works [17-19] we reported that high-Mn austenitic steels showed higher corrosion current density during potentiodynamic polarization tests in 0.1M H_2SO_4 than in 3.5% NaCl solution. Opiela et al. [20] observed the presence of numerous corrosion pits formed in steels after corrosion tests in both solutions. Better corrosion resistance of high-Mn steels in 3.5% NaCl is related to the passivation ability of aluminium, i.e., formation of stable Al_2O_3 films on the steel surface in solution characterized by pH about 7. The lowest corrosion resistance of investigated steels in acidic solution can be explained by non-passivating tendency of aluminium in this medium in addition to the intensive manganese and iron dissolution.

Heat treatment conditions and plastic deformation have also a significant effect on microstructure and mechanical properties of steels [21-24]. Up to now a lot of studies on AHSS steels concerned their hot-working behavior [6,25-30]. Less attention has been focused on relations between a type of heat treatment, plastic deformation and corrosion properties of high-Mn steels. Nowadays, a few reports on relations between cold deformation of high-Mn steels and their corrosion resistance are available [18,31,32]. Ghayad et al. [31] found that cold working increases the corrosion rate due to deformation twins formed upon deformation. The twins represent regions characterized by different potential from the matrix and this leads to the increase in the corrosion current density. Results of our previous works [9,10] confirmed that corrosion pits nucleated mainly at grain boundaries and deformation bands in cold deformed steels. Corrosion resistance of grain boundaries is poor because of high dislocation density present at these regions [17,33]. The same effect was observed in stainless steels [34]. Grain size influences the corrosion behaviour too. A result of the plastic deformation can be the formation of ε or/and α' martensites. It was reported [32,35] that the corrosion progress is accelerated when the amount of the martensite increases.

This study contains comparative investigations of the corrosion properties of two high-Mn steels in three different states (hot deformed, supersaturated and cold strained) in 0.1M NaOH.

2. Experimental

Examinations were carried out on two vacuum-melted high-Mn steels with the chemical composition presented in Table 1. The steels are characterized by similar C and Mn content (major austenite stabilizers). The main differences in chemical composition of investigated steels are related to the silicon and aluminium contents. The chemical behaviour of those elements is opposite. Aluminium can improve corrosion resistance of steel due to the passive film forming tendency on a steel surface, whereas silicon

addition has a negative effect on corrosion resistance of steels [7,8,15].

Table 1.
Chemical composition of the investigated steels

Compo-nent	Mass contents, %	
	X6MnSiAlNbTi26-3-3	X4MnSiAlNbTi27-4-2
C	0.065	0.040
Mn	26.0	27.5
Si	3.08	4.18
Al	2.87	1.69
P	0.002	0.004
S	0.013	0.017
Nb	0.034	0.033
Ti	0.010	0.010
N	0.0028	0.0028
O	0.0006	0.0006

The investigated steels were obtained in a rolling process using the thermomechanical treatment. The ingots were hot-forged and subsequently rolled to a thickness of 4.5 mm. The thermomechanical rolling included 3 passes (rolling reductions: 25%, 25% and 20%) to a final sheet thickness of app. 2 mm obtained at the finishing rolling temperature of 850°C. Next, the samples were rapidly cooled in water to room temperature. Three groups of specimens were prepared:

1. thermomechanically rolled,
2. thermomechanically rolled and subsequently annealed at 900°C for 20 min,
3. thermomechanically rolled and subsequently cold deformed in static tensile test to total elongation of 36%.

Microstructures were examined by Zeiss Axio Observer Z1m optical microscope. All samples were ground using 400-1200-grit SiC paper, polished with Al_2O_3 with granularity of 0.1 µm and then etched using 5% nital to reveal the microstructure.

Corrosion resistance of the investigated steels was examined using potentiodynamic method. The corrosion behaviour of the thermomechanically processed specimens was compared to supersaturated and cold worked specimens. Corrosion tests were carried out in 0.1M NaOH solution (pH~14) on samples with an area of about 0.38 cm^2. The working area of the specimens was mechanically ground with 1200-grit SiC paper. Then, the samples were polished with Al_2O_3 of 0.1 µm granularity. The samples were washed in distilled water and rinsed in acetone prior to tests. All corrosion tests were conducted at ambient temperature. Polarization studies were carried out using an Atlas 0531 Electrochemical Unit potentiostat/galvanostat driven by AtlasCorr05 software and an electrochemical corrosion cell consisting of a specimen as a working electrode, stainless steel as a counter electrode and silver/silver chloride (Ag/AgCl) reference electrode (Fig. 1). The solution concentration inside the standard silver electrode (SSE) was 3 M KCl, with a potential of 0.22 V with respect to hydrogen. A scan rate of 1 mV/s was employed during polarization. Potentiodynamic scan data were collected to determine the electrochemical parameters: corrosion potential E_{corr} and corrosion current I_{corr}.
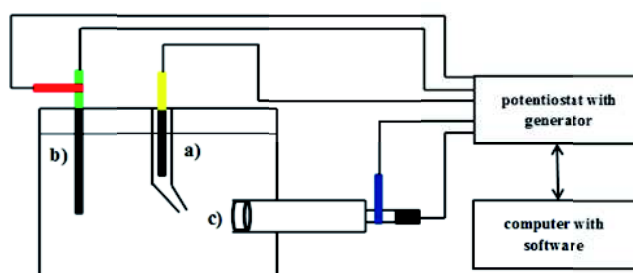

Fig. 1. Schematic representation of the three-electrode configuration used for the experiment: silver/silver chloride (Ag/AgCl) reference electrode (a), stainless steel counter electrode (b), specimen – working electrode (c)

For scanning electron microscopy (Zeiss SUPRA 25) all samples after corrosion tests were polished using Al_2O_3 with granularity of 0.1 µm, then cleaned with distilled water and etched in 5% nital to reveal initiation sites of potential pits. Corrosion damage was examined by SEM observations and EDS technique.

3. Results

The microstructures of X6MnSiAlNbTi26-3-3 and X4MnSiAlNbTi27-4-2 steels in their different states are shown in Figs. 2-4. The microstructures of both thermomechanically treated specimens (Figs. 2a,b) are characterized by relatively coarse austenite grains (grain size estimated as 80 µm), elongated according to hot rolling direction. The microstructures reveal the presence of annealing twins and elongated sulfide inclusions.

Figure 3 shows the optical micrograph of the X4MnSiAlNbTi27-4-2 solution-treated specimen. The microstructure is characterized by a bimodal distribution of grains (grain size estimated as 40 µm). Relatively large elongated austenite grains and small recrystallized grains can be observed.
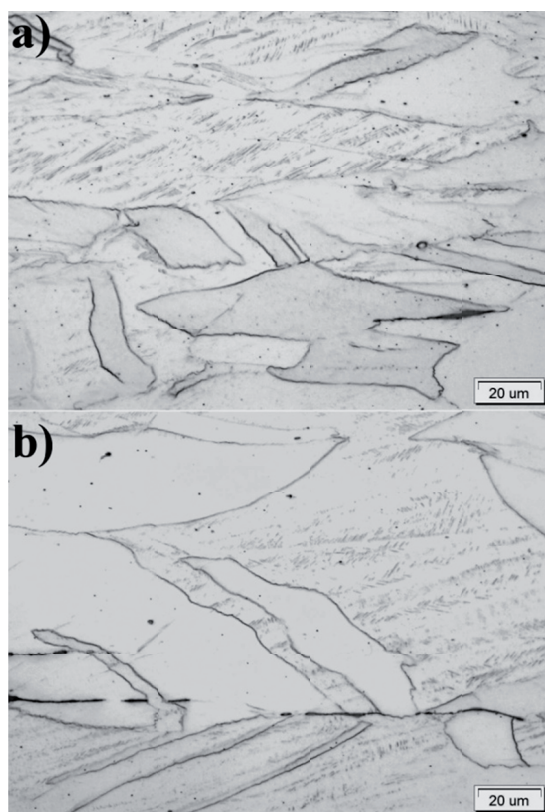
Fig. 2. Austenitic microstructure of the thermomechanically rolled X4MnSiAlNbTi27-4-2 (a) and X6MnSiAlNbTi26-3-3 (b) steels
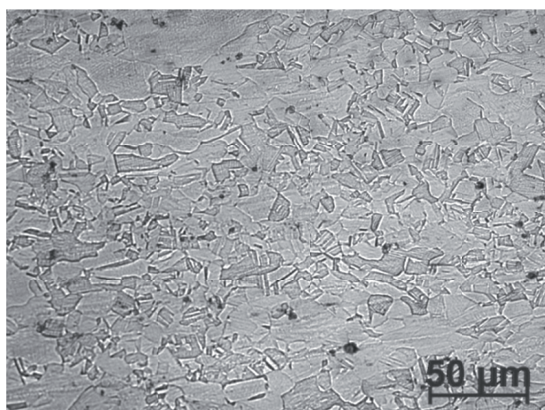

Fig. 3. Austenitic microstructure of the X4MnSiAlNbTi27-4-2 solution-treated steel

The micrographs in Fig. 4a and Fig. 4b show the X6MnSiAlNbTi26-3-3 and X4MnSiAlNbTi27-4-2 steels after the tensile test performed at room temperature to the 36% strain. The elongated austenite grains and numerous slip bands can be observed. Additionally, the high amount
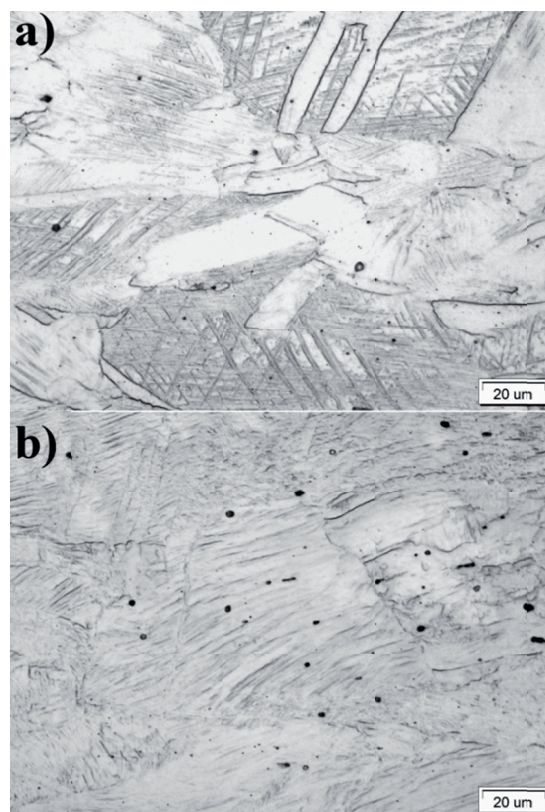

Fig. 4. Austenitic microstructure of the cold deformed X4MnSiAlNbTi27-4-2 (a) and X6MnSiAlNbTi26-3-3 (b) steels

of deformation twins and presence of elongated sulfide inclusions were identified.

The electrochemical measurements were conducted to determinate the effect of heat treatment and deformation on the corrosion resistance of high-Mn steels in alkaline solution (0.1M NaOH). Additionally, the effect of non-metallic inclusions on pitting corrosion behaviour was investigated. Selected results of potentiodynamic polarization measurements obtained for both steels in different states of treatment are shown in Figs. 5 and 6. In order to determine the corrosion current (I_{corr}) and corrosion potential (E_{corr}) the Tafel slope extrapolation method was used. Results of the measurements are shown in Table 2.

Potentiodynamic polarization data obtained for thermo-mechanically treated steels are shown in Fig. 5a. The X4MnSiAlNbTi27-4-2 steel showed slightly higher corrosion current density (0.007 mA/cm^2), when compared to the steel containing higher aluminium content – 0.005 mA/cm^2. It is in accordance with our earlier results of potentiodynamic polarisation tests [9]. The corrosion potential values of both thermomechanically treated steels

Table 2.
Average values of electrochemical polarization data of thermomechanically rolled, supersaturated and cold worked steels registered in the 0.1M NaOH solution

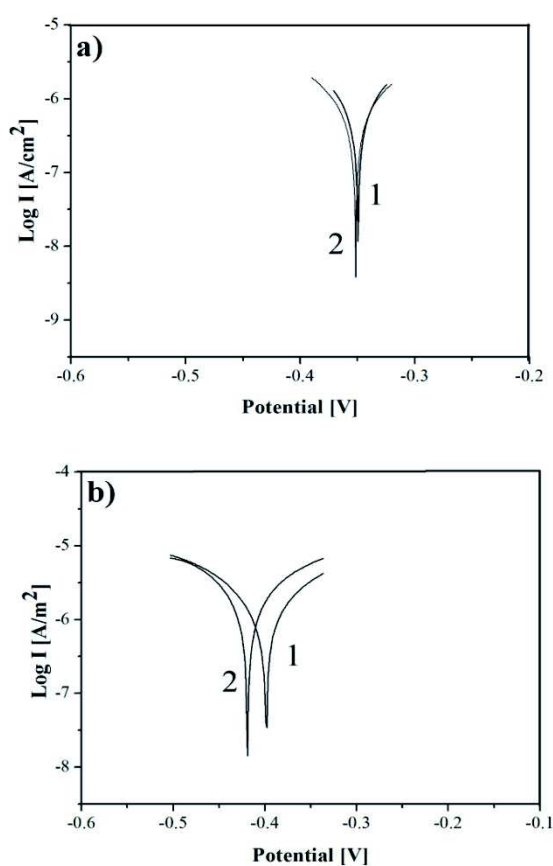| Material	Type of treatment	0.1M NaOH	
		E_{corr} mV	I_{corr} mA/cm^2
X4MnSiAlNbTi 27-4-2	thermomechanically rolled	-355	0.007
X6MnSiAlNbTi 26-3-3	thermomechanically rolled	-352	0.005
X4MnSiAlNbTi 27-4-2	supersaturated	-430	0.03
X4MnSiAlNbTi 27-4-2	cold worked	-398	0.09
X6MnSiAlNbTi 26-3-3	cold worked	-420	0.06

Fig. 5. Selected potentiodynamic polarization curves of the thermomechanically treated (a) and cold deformed (b) X4MnSiAlNbTi27-4-2 (1) and X6MnSiAlNbTi26-3-3 (2) steels registeted in 0.1M NaOH solution
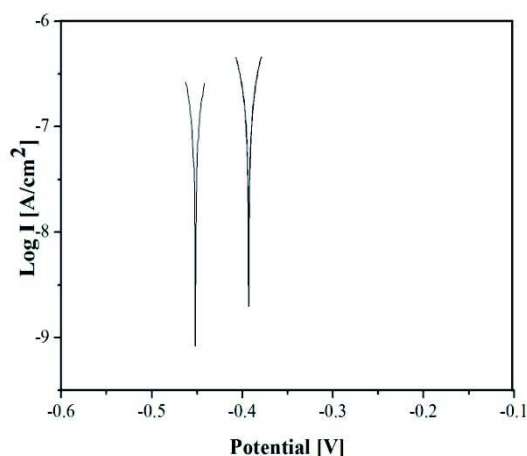
Fig. 6. Selected potentiodynamic polarization curves of the supersaturated X4MnSiAlNbTi27-4-2 steel obtained in 0.1M NaOH solution
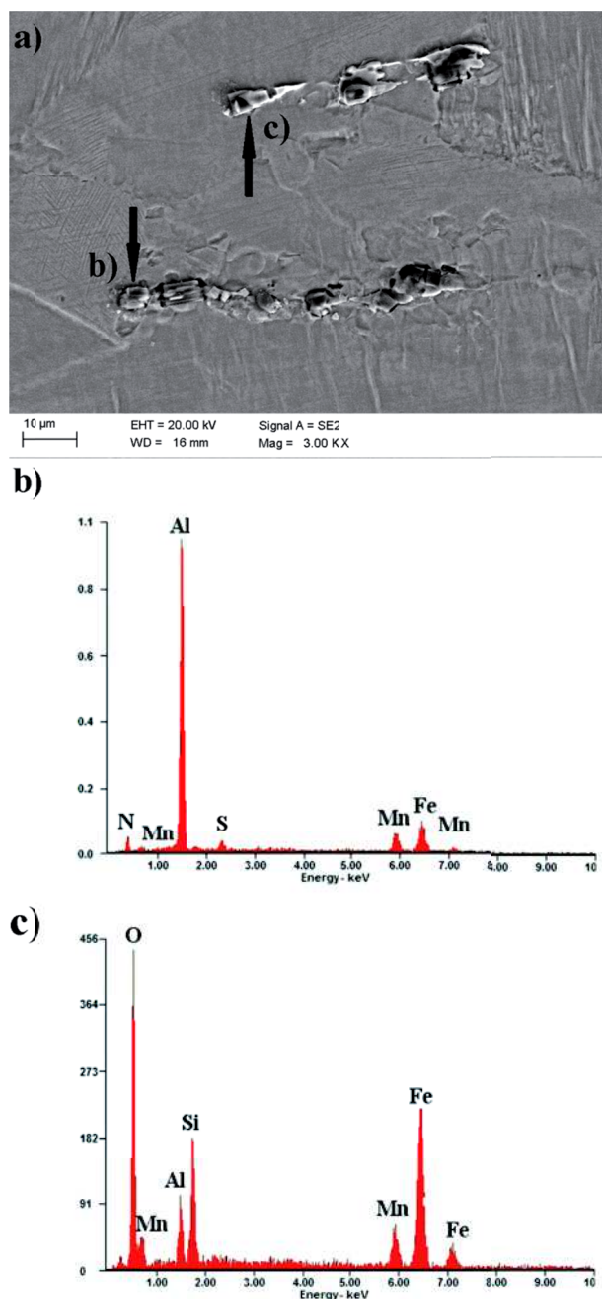
were: -355 mV and -352 mV respectively for X4MnSiAl-NbTi27-4-2 and X6MnSiAlNbTi26-3-3 steels.

Results collected for cold deformed specimens are shown in Fig. 5b. Cold deformation increased the corrosion current density to approximately 0.09 mA/cm^2 – for the 27-4-2 steel and to 0.06 mA/cm^2 for the 26-3-3 steel. The values of corrosion potentials were: -398 mV and -420 mV for the steels containing lower and higher Al content, respectively. It is documented in literature [17-19,31,32, 36,37] that in general, cold deformation decreases corrosion resistance of steels. It is reflected in higher values of corrosion current density (I_{corr}).

A bimodal distribution of grains had a negative influence on corrosion resistance of the X4MnSiAlNbTi27-4-2 steel. Supersaturated specimens showed a mean value of corrosion current density of about 0.03 mA/cm^2 (Fig. 6). The mean value of corrosion potential was about -430 mV.

Pitting behaviour was studied by SEM and EDS techniques. Selected results of the analysis are shown in Figs. 7 and 8. A number of corrosion pits formed in the thermomechanically treated X4MnSiAlNbTi27-4-2 steel was quite small. They were mostly distributed at grain boundaries. A few pits are located within the austenite grains (Fig. 7a). Results of EDS analysis revealed that corrosion pits initiated at single MnS, AlN and at complex MnS+AlN inclusions (Fig. 7b). Corrosion pits nucleated also at complex oxides containing Mn, Al and Si (Fig. 7c).

The cold deformed X6MnSiAlNbTi26-3-3 steel possessed single and complex inclusions consisting of MnS and AlN too. SEM observation revealed that corrosion damages are distributed at grain boundaries, inside the austenite grains and along the deformation bands. The amount

Fig. 7. SEM micrograph of the surface of thermomecha-nically treated X4MnSiAlNbTi27-4-2 steel (a); the EDS analysis of the individual pit interior revealed the compo-sition of the inclusion as follows (in wt. %): point (b) – Al (52.9%), N (14.9%), Mn (9.6%), S (2.5%) and point (c) – O (27.4%), Si (9.9%), Mn (9.3%), Al (5.1%)

of corrosion pits nucleated at steel's surface as a result of reaction between surface of cold deformed steel in 0.1M NaOH solution is slightly higher than observed for
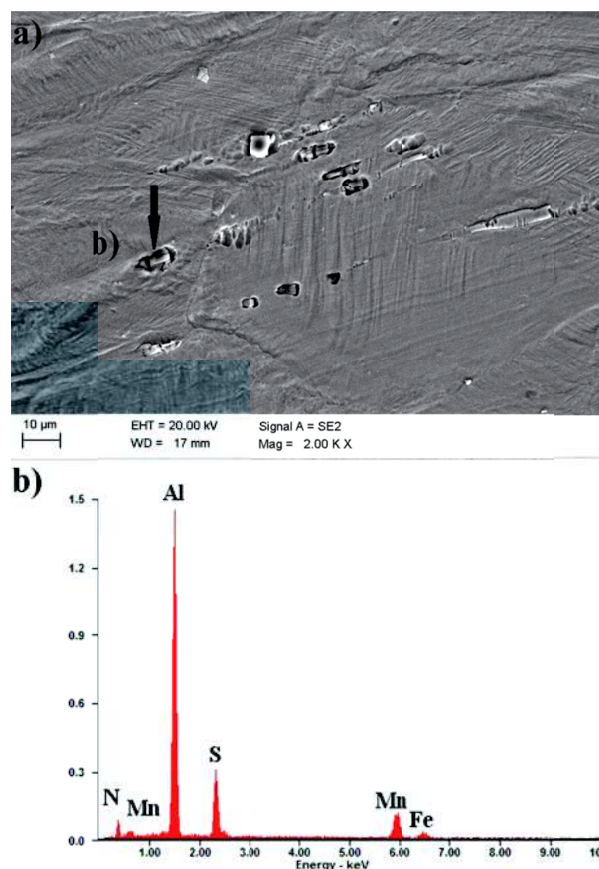

Fig. 8. SEM micrograph of the surface of cold deformed X6MnSiAlNbTi26-3-3 steel (a). EDS analysis of the individual pit interior (b) revealed the composition of the inclusion as follows: Al (46.9 wt. %), Mn (18.0 wt. %), N (17.6 wt. %), S (14.2 wt. %)

thermomechanically treated specimens (Fig. 8a). Similar results were observed for the cold deformed X6MnSiAl-NbTi26-3-3 steel after corrosion test in 3.5% NaCl solution [10]. The EDS analysis indicated the high content of manganese, sulphur, aluminium and nitrogen inside the individual corrosion pits (Fig. 8b). It indicates that in this case, the privileged places for the pit initiation are MnS and AlN (single and complex) inclusions too. There are many reports in literature [9-13], which confirm a negative effect of non-metallic inclusions (especially MnS) on the corro-sion properties of steels.

4. Discussion

It is evident from this work that the presented poten-tiodynamic parameters (Table 2): corrosion current (I_{corr})

and corrosion potential (E_{corr}) measured for both steels are related to several factors, such as: chemical composition of steel, heat treatment and plastic deformation.

Chemical composition of steel, especially metallurgical cleanliness related to the amount of non-metallic inclusions, has a significant effect on its corrosion resistance. Previous studies [10-13] demonstrated that non-metallic inclusions, mostly sulfide inclusions, affect the corrosion resistance of steel by providing pitting sites. That way, special focus should be paid to controlling the amount of sulfur content during metallurgical processes. Results of our earlier study [38] showed that X4MnSiAlNbTi27-4-2 steel possesses a higher sulfur content (0.017 wt.%) than X6MnSiAlNbTi26-3-3 steel – 0.013 wt.%. The higher sulfur content can also affect the corrosion resistance of steel. The mean value of corrosion current density detected for the steel containing a lower Al amount was higher than that one recorded for X6MnSiAlNbTi26-3-3 steel (Table 2).

The amount of MnS inclusions depends primarily on the sulfur content, thus the lower corrosion resistance of X4MnSiAlNbTi27-4-2 steel was observed. Park and Kwon [39] found that a size of MnS inclusions increased with the increase of Mn concentration in Fe-18Cr-6Mn and Fe-18Cr-12Mn steels. Therefore, corrosion behaviour of the steel with lower Al content could be also accelerated (to a lesser extend) by the higher Mn content in this steel. It is reported that [11,40] AlN inclusions are characterized by higher corrosion resistance than MnS inclusions. Results of EDS analysis showed that AlN inclusions were present in both steels. The X6MnSiAlNbTi26-3-3 steel is characterized by higher Al content. Thus, better corrosion resistance of this steel can be also probably related to higher amount of AlN inclusions (and smaller quantity of MnS inclusions). Based on our previous results of potentiodynamic tests [9,10] it can be observed that corrosion pits did not form on Al_2O_3 inclusions during corrosion tests in 0.1M NaOH in opposite to 3.5% NaCl solution. Park et . al. [40] reported that Al_2O_3 inclusions have better corrosion resistance than MnS and AlN inclusions. Therefore, it can be concluded that 0.1M NaOH is less aggressive corrosion solution for high-Mn steels. Better corrosion resistance of the X6MnSiAlNbTi26-3-3 steel is attributed to higher Al and lower Si contents in comparison to the X4MnSiAlNbTi27-4-2 steel (Table 2).

A type of heat treatment and cold deformation influence the corrosion behavior of steel. Corrosion pits usually are formed in places of high dislocation density: grain boundaries, twins and deformation bands. These regions are particularly vulnerable for pit nucleation. The larger amount of deformation twins present in the microstructure of the cold deformed steels contributes to lowering their corrosion resistance due to the difference in potentials between the matrix and twins. They create local corrosion cells. That is why the cold deformed specimens were characterized by higher corrosion current density in comparison to the thermomechanically processed specimens.

Di Schino et al. [33] and Abbasi Aghuy et al. [34] reported that corrosion resistance of steel is also related to its grain size. The grain refinement may change the electrochemical behaviour of metal as a consequence of variation in grain boundary density. Ralston et al. [41] suggested that the impact of grain refinement on corrosion resistance depends on the ability of surface to passivation. For the active conditions, reduction in the alloy grain size deteriorates the corrosion resistance whereas in an environment at which passivity could be established, grain refinement causes the improvement of corrosion resistance. Abbasi Aghuy et al. [34] observed that in austenitic 304L stainless steel pitting potential is not affected by grain refinement. Moreover, grain refinement decreases the number of corrosion pits. Relatively lower frequency of pits formation was explained based on the ability of grain boundaries to form a more strong passive film. More fine-grained 304L steel has a high density of grain boundaries for forming passive layers containing more chromium. Results of the present experiments indicated that thermomechanically rolled samples showed higher corrosion resistance than supersaturated specimens. The highest mean value of corrosion current density I_{corr} was detected for cold deformed specimens. Di Schino et al. [33] observed that in stainless steel a pitting corrosion rate decreased with decreasing grain size, while the uniform corrosion resistance is impaired by grain refining. Based on previous reports [33,34] it can be concluded that a dominant type of corrosion of investigated high-Mn steels in 0.1M NaOH solution is uniform corrosion without passivation. The general corrosion is accompanied by a small number of corrosion pits.

5. Conclusions

Corrosion behaviour of high-Mn austenitic steels is a complex problem related to numerous material and processing factors. The effects of chemical composition and plastic deformation on the corrosion properties in alkaline (0.1M NaOH) solution were studied. The following conclusions can be drawn:

- both X4MnSiAlNbTi27-4-2 and X6MnSiAlNbTi26-3-3 steels of different Al and Si contents were characterized

by relatively high corrosion resistance in 0.1M NaOH, independently of their state: solution-treated, thermomechanically rolled, cold strained;

- corrosion pits nucleating preferentially on single and complex non-metallic inclusions consisting of MnS and AlN accelerate the uniform corrosion;
- corrosion resistance of high-Mn steels is related to the type and amount of non-metallic inclusions. The higher contents of manganese, sulfur and silicon combined with a lower content of aluminium is reflected in the worse corrosion resistance of the X4MnSiAlNbTi27-4-2 steel;
- corrosion damages were distributed mostly at grain boundaries and within deformation bands;
- cold deformation had the highest effect on the reduction of corrosion resistance of investigated steels. Thermomechanically treated and supersaturated specimens showed lower values of corrosion current density and consequently less amount of corrosion damage.

References

[1] O. Grässel, L. Krüger, G. Frommeyer, L.W. Meyer, High strength Fe-Mn (Al,Si) TRIP/TWIP steels developments properties – applications, International Journal of Plasticity 16 (2000) 1391-1409.

[2] J. Mazurkiewicz, Structure and properties of high manganese MnSiAlNbTi25-1-3 steels with increased store of cold plastic deformation energy, Open Access Library 7/25 (2013) 1-139 (in Polish).

[3] A. Grajcar, M. Opiela, G. Fojt-Dymara, The influence of hot-working conditions on a structure of high-manganese steel, Archives of Civil and Mechanical Engineering 9/3 (2009) 49-58.

[4] G. Frommeyerr, U. Brux, Microstructures and mechanical properties of high-strength Fe-Mn-Al-C light TRIPLEX Steels, Steel Research International 77 (2006) 627-633.

[5] L.A. Dobrzański, A. Grajcar, W. Borek, Microstructure evolution of C-Mn-Si-Al-Nb high-manganese steel during the thermomechanical processing, Materials Science Forum 638-642 (2010) 3224-3229.

[6] L.A. Dobrzański, W. Borek, Hot deformation and recrystallization of advanced high-manganese austenitic TWIP steels, Journal of Achievements in Materials and Manufacturing Engineering 46/1 (2011) 71-78.

[7] Y.S. Zhang, X.M. Zhua, S.H. Zhong, Effect of alloying elements on the electrochemical polarization behavior and passive film of Fe–Mn base alloys in various aqueous solutions, Corrosion Science 46/4 (2004) 853-876.

[8] T. Dieudonné, L. Marchetti, M. Wery, F. Miserque, M. Tabarant, J. Chêne, C. Allely, P. Cugy, C.P. Scott, Role of copper and aluminum on the corrosion behavior of austenitic Fe–Mn–C TWIP steels in aqueous solutions and the related hydrogen absorption, Corrosion Science 83 (2014) 234-244.

[9] A. Grajcar, A. Płachcińska, Effect of sulphide inclusions on the pitting corrosion behavior of high-Mn steels in chloride and alkaline solutions, Materiali in Tehnologije 50/5 (2016) (in press).

[10] A. Grajcar, B. Grzegorczyk, A. Kozłowska, Corrosion resistance and pitting behaviour of low-carbon high-Mn steels in chloride solution, Archives of Metallurgy and Materials 61 (2016) (in press).

[11] P. Schmuki, H. Hildebrand, A. Friedrich, S. Virtanen, The composition of the boundary region of MnS inclusions in stainless steel and its relevance in triggering pitting corrosion, Corrosion Science 47 (2005) 1239-1250.

[12] D.E. Williams, M. R. Kilburn, J. Cliff, G.I.N. Waterhouse, Composition changes around sulphide inclusions in stainless steels, and implications for the initiation of pitting corrosion, Corrosion Science 52 (2010) 3702-3716.

[13] H. Krawiec, V. Vignal, O. Heintz, R. Oltra, Influence of the dissolution of MnS inclusions under free corrosion and potentiostatic conditions on the composition of passive films and the electrochemical behaviour of stainless steels, Electrochimica Acta 51 (2006) 3235-3243.

[14] S. Lasek, E. Mazancova, Influence of thermal treatment on structure and corrosion properties of high manganese TRIPLEX steels, Metalurgija 52/4 (2013) 441-444.

[15] M.B. Kannan, R.K.S. Raman, S. Khoddam, Comparative studies on the corrosion properties of a Fe-Mn-Al-Si steel and an interstitial-free steel, Corrosion Science 50/10 (2008) 2879-2884.

[16] V.F.C. Lins, M.A. Freitas, E.M.P. e Silva, Corrosion resistance study of Fe–Mn–Al–C alloys using immersion and potentiostatic tests, Applied Surface Science 250/1-4 (2005) 124-134.

[17] A. Grajcar, A. Płachcińska, S. Topolska, M. Kciuk, Effect of thermomechanical treatment on the corrosion behaviour of Si and Al-containing high-Mn austenitic steel with Nb and Ti microaddition, Materiali in Tehnologije 49/6 (2015) 889-894.

[18] A. Grajcar, A. Płachcińska, M. Kciuk, S. Topolska, Microstructure and electrochemical behaviour of hot-deformed and cold-strained high-Mn steels, Journal of Materials Engineering and Performance 25 (2016) (in press).

[19] A. Grajcar, S. Kołodziej, W. Krukiewicz, Corrosion resistance of high-manganese austenitic steels, Archives of Materials Science and Engineering 41/2 (2010) 77-84.

[20] M. Opiela. A. Grajcar, W. Krukiewicz, Corrosion behaviour of Fe-Mn-Si-Al austenitic steel in chloride solution, Journal of Achievements in Materials and Manufacturing Engineering 33/2 (2009) 159-165.

[21] J. Adamczyk, A. Grajcar, Effect of heat treatment conditions on the structure and mechanical properties of DP-type steel, Journal of Achievements in Materials and Manufacturing Engineering 17 (2006) 305-308.

[22] A. Grajcar, M. Opiela, Influence of plastic deformation on CCT-diagrams of low-carbon and medium-carbon TRIP steels, Journal of Achievements in Materials and Manufacturing Engineering 29 (2008) 71-78.

[23] M. Jabłońska, A. Śmiglewicz, A study of mechanical properties of high manganese steels after different rolling conditions, Metalurgija 54/4 (2015) 619-622.

[24] M. Jabłońska, R. Michalik, Studies on the corrosion properties of high-Mn austenitic steels, Solid State Phenomena 227 (2014) 75-78.

[25] L.A. Dobrzański, W. Borek, Thermo-mechanical treatment of Fe–Mn–(Al, Si) TRIP/TWIP steels, Archives of Civil and Mechanical Engineering 12/3 (2012) 299-304.

[26] M. Opiela, A. Grajcar, Hot deformation behavior and softening kinetics of Ti-V-B microalloyed steels, Archives of Civil and Mechanical Engineering 12/3 (2012) 327-333.

[27] A. Grajcar, Structural and mechanical behaviour of TRIP-type microalloyed steel in hot-working conditions, Journal of Achievements in Materials and Manufacturing Engineering 30 (2008) 27-34.

[28] A. Grajcar, Effect of hot-working in the $\gamma+\alpha$ range on a retained austenite fraction in TRIP-aided steel, Journal of Achievements in Materials and Manufacturing Engineering 22 (2007) 79-82.

[29] T. Bator, Z. Muskalski, S. Wiewiórowska, J.W. Pilarczyk, Influence of the heat treatment on the mechanical properties and structure of TWIP steel in wires, Archives of Materials Science and Engineering 28/6 (2007) 337-340.

[30] A. Grajcar, Determination of the stability of retained austenite in TRIP-aided bainitic steel, Journal of Achievements in Materials and Manufacturing Engineering 20 (2007) 111-114.

[31] I.M. Ghayad, A.S. Hamada, N.N. Girgis, W.A. Ghanem, Effect of cold working on the aging and corrosion behaviour of Fe-Mn-Al stainless steel, Steel Grips 4 (2006) 133-137.

[32] A. Grajcar, W. Krukiewicz, S. Kołodziej, Corrosion behaviour of plastically deformed high-Mn austenitic steels, Journal of Achievements in Materials and Manufacturing Engineering 43/1 (2010) 228-235.

[33] A. Di Schino, M. Barteri, J.M. Kenny, Grain size dependence of mechanical, corrosion and tribological properties of high nitrogen stainless steels, Journal of Materials Science 38/15 (2003) 3257-3262.

[34] A. Abbasi Aghuy, M. Zakeri, M.H. Moayed, M. Mazinani, Effect of grain size on pitting corrosion of 304L austenitic stainless steel, Corrosion Science 94 (2015) 368-376.

[35] Y.S. Chun, J.S. Kim, K.T. Park, Y.K. Lee, C.S. Lee, Role of ε martensite in tensile properties and hydrogen degradation of high-Mn steels, Materials Science and Engineering A 533 (2012) 87-95.

[36] Y. Fu, X. Wu, E.H. Han, W. Ke, K. Yang, Z. Jiang, Effects of cold work and sensitization treatment on the corrosion resistance of high nitrogen stainless steel in chloride solutions, Electrochimica Acta 54 (2009) 1618-1629.

[37] A. Kurc, M. Kciuk, M. Basiaga, Influence of cold rolling on the corrosion resistance of austenitic steel, Journal of Achievements in Materials and Manufacturing Engineering 38/2 (2010) 154-162.

[38] A. Grajcar, U. Galisz, L. Bulkowski, Non-metallic inclusions in high manganese austenitic alloys, Journal of Achievements in Materials and Manufacturing Engineering 50/1 (2011) 21-30.

[39] K.J. Park, H.S. Kwon, Effects of Mn on the localized corrosion behavior of Fe–18Cr alloys, Electrochimica Acta 55 (2010) 3421-3427.

[40] J. Park, S.M. Lee, M. Kang, S. Lee, Y.K. Lee, Pitting corrosion behavior in advanced high strength steels, Journal Alloy and Compounds 619 (2015) 205-210.

[41] K.D. Ralston, N. Birbilis, Effect of grain size on corrosion: a review, Corrosion 66/7 (2010) 5-13.